Homologous Phases Built by Boron Clusters and Their Vibrational Properties

Fuxiang Zhang, Fangfang Xu, Andreas Leithe-Jasper,[†] Takao Mori, Takaho Tanaka,* Jun Xu, Akira Sato, Yashio Bando, and Yashio Matsui

National Institute for Materials Science, Advanced Materials Laboratory, Namiki 1-1, Tsukuba, Ibaraki 305-0044, Japan

We have found a series of new rare earth boron-rich solids in REBC(N) (RE: Y, Ho, Er, Tm, and Lu), systems and their structures are solved from single crystal and/or powder X-ray diffraction data. Structure analysis results show that they are homologous with B_4C and also show trigonal symmetry. As the two basic structural units, boron icosahedra and octahedra in the new phases form in layers and stack in different sequences which form different phases. With increasing number of icosahedral layers stacking between two neighboring octahedral layers, the *c*-axis of the unit cell is increased and the other two edges of the unit cell are only changed slightly. Three monophases of the series have been synthesized both in powders and as single crystals. The vibrational modes of the homologous phases are analyzed from the Raman spectra and compared with that of B_4C.

Introduction

Boron-rich solids hold a special place within chemistry and materials. They do not follow the general bonding rules, and the boron atoms usually bond in very stable clusters, such as the 12-atom cluster of the icosahedron and the 6-atom cluster of the octahedron. These molecular-like solids display an amazing array of "anomalies" in their electronic, magnetic, and thermal properties.[1−3] Boron carbide, B_4C, has already suggested an application as a very high temperature thermoelectric material[1] (stable up to 1800 K). In addition, B_4C is also a superhard material just after diamond and cubic BN. Unlike boron suboxide[4] (B_6O), B_4C is rather easy to prepare even for bulk single crystals. Here we report the finding of a series of new compounds in rare earth boron carbon and/or nitrogen systems, in which boron icosahedra and octahedra build homologous phases and the structure is similar to that of B_4C. Homologous structures have been found in the quaternary intermetallic compounds of LuNiBC (ref 5) and LaNiBN (ref 6) which show superconducting properties for some phases. However, this is the first observation of homologous structures built by different boron clusters in boron-rich solids. Their vibrational properties have been measured with Raman spectra and compared with those of B_4C.

The crystal structure of B_4C is composed of six distorted $B_{11}C$ icosahedra located at the apexes of a rhombohedral Bravais lattice in the $R\bar{3}m$ space group. This is a modification of the α-boron structure, where a three-atom chain of C−B−C resides at the center of the unit cell and along the (111) rhombohedral axis, linking different $B_{11}C$ icosahedra.[7−8] In a trigonal unit cell, the crystal structure can be understood as a stacking of icosahedral layers perpendicular to the *c*-axis and C−B−C chains parallel to the *c*-axis and linking the icosahedra in neighboring layers (Figure 1d).

Experimental Section

During our investigation in rare earth boron carbon and/or nitrogen systems with solid state reaction methods, we have found that the icosahedral layers in B_4C can be replaced with boron octahedral layers under certain rules. The boron octahedron is smaller than the icosahedron in size, so rare earth atoms can reside in the voids of the replaced layers. The three monophases of $REB_{15.5}C_{2−x}N_x$, $REB_{22}C_{3−x}N_x$ ($0 \le x \le 1$), and $REB_{28.5}C_4$ were obtained in the ternary and quaternary systems with rare earth atoms of Y, Ho, Er, Tm, and Lu both in powders and as single crystals. The compositions of RE and B in the powder samples were determined by an inductively coupled plasma atomic emission spectroscopy analysis after the samples were dissolved into a concentrated HNO_3 + concentrated HCl (1:1) solution by keeping them in an airtight vessel at 110 °C for about 12 h. The carbon content was determined by a volumetric combustion method using a carbon determinator (LECO CS-444), and nitrogen was determined with a standard inert gas fusion method (LECO TC-436AR). The first phase can also be obtained in Sc−B−C−N quaternary system.[9] Powder is synthesized by solid state reaction[10] in a RF furnace with BN crucibles and a graphite susceptor at a temperature of 1700 °C or so. The starting materials were amorphous B, pure carbon, and rare earth borides such as YB_4 and other rare earth borides of REB_n prepared by a boron thermal reduction method[10] from the corresponding oxides. For some samples including N, BCN precursor, which was prepared from urea, boric acid, and saccarose at 1400 °C for 2 h, was used. Single crystals were prepared by a high-temperature solution growth method using copper or tin as the flux. All the structures of single phases were solved from X-ray diffraction data of single crystal and/or powders with direct methods. Details of the individual structure analysis were published elsewhere.[11−12] The structure models were refined with least-squares methods and confirmed by TEM observations.

* Corresponding author. E-mail: TANAKA.Takao@nims.go.jp.
† Present address: MPI-CPFS, Bayreuther Strasse 40, Dresden, D-01187, Germany.

(1) Emin, D. *Phys. Today* **1987**, January, 55.
(2) Young, D. P.; Hall, D.; Torelli, M. E.; Fisk, Z.; Sarrao, J. L.; Thompson, J. D.; Ott, H.-R.; Oseroff, S. B.; Googrich, R. G.; Eysler, R. *Nature* **1999**, *397*, 412.
(3) Nyhus, P.; Cooper, S. L.; Fisk, Z.; Sarrao, J. L. *Phys. Rev.* **1997**, *B55*, 12488.
(4) Hubert, H.; Devouard, B.; Garvie, L. A. J.; O'keeffe, M.; Buseck, P. R. B.; Petusky, W. T.; McMillan, P. F. *Nature* **1998**, *391*, 376.
(5) Siegrist, T.; Zandbergen, H. W.; Cava, R. J.; Krajewski, J. J.; Peck, W. F., Jr. *Nature* **1994**, *367*, 254.
(6) Zandbergen, H. W.; Jansen, J.; Cava, R. J.; Krajewski, J. J.; Peck, W. F., Jr. *Nature* **1994**, *372*, 759.

(7) Kwei, G. H.; Morosin, B. *J. Phys. Chem.* **1996**, *100*, 8031.
(8) Emin, D. *Phys. Rev.* **1988**, *B38*, 6041.
(9) Leithe-Jasper, A.; Tanaka, T.; Bourgeois, L.; Bando, Y. *J. Solid State Chem.*, in press.
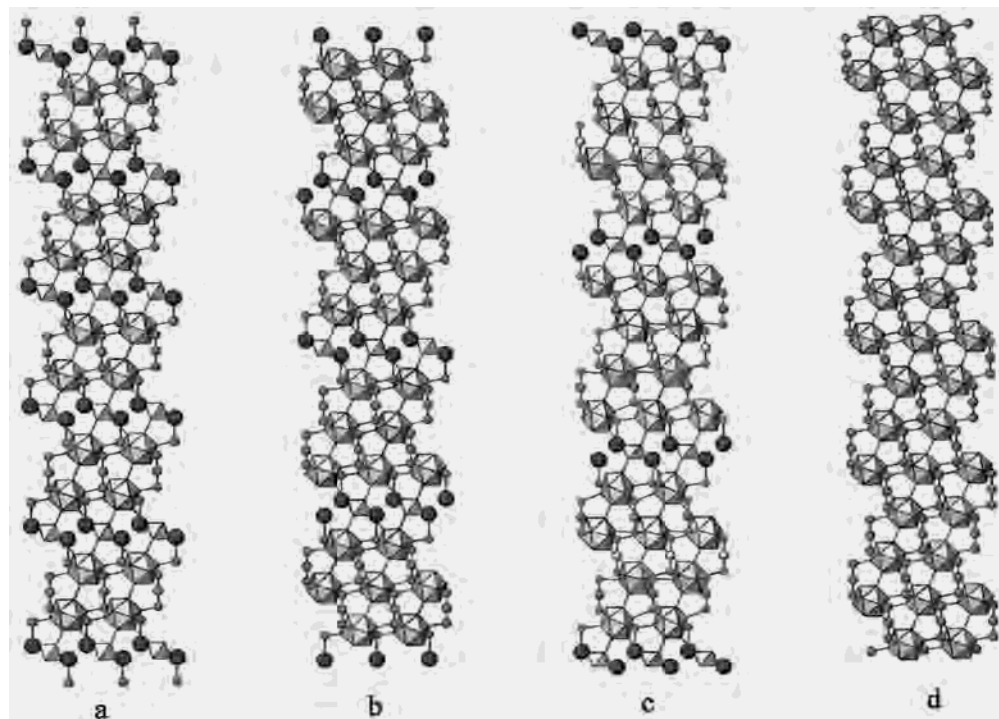(10) Tanaka, T.; Okada, S.; Ishizawa, Y. *J. Alloys Compd.* **1994**, *205*, 281.

Figure 1. Schematic drawing of crystal structures of the homologous phases of (a) 3T, (b) 12R, (c) 15R, and (d) B_4C. The large and small polyhedra are boron icosahedra and octahedra, respectively; the large balls are rare earth atoms, and small ones bonded with them are C or N (for 3T and 12R phases). The three bonded atoms parallel to the c-axis are C−B−C chains.

Table 1. Structural Parameters of the Homologous Phases 3T, 12R, and 15R

phase	formula	Z^a	space group	a, c (Å)	V (Å^3)	atoms^b
3T	$YB_{15.5}CN$	3	$P\bar{3}m1$ (No. 164)	5.592, 10.873	294.9	9
	$HoB_{15.5}CN$			5.588, 10.878	294.2	
	$ErB_{15.5}CN$			5.589, 10.880	294.3	
	$TmB_{15.5}CN$			5.580, 10.850	292.6	
	$LuB_{15.5}CN$			5.577, 10.839	291.9	
12R	$YB_{22}C_3$	6	$R\bar{3}m$ (No. 166)	5.623, 44.765	1226.9	12
	$HoB_{22}C_3$			5.614, 44.625	1248.4	
	$ErB_{22}C_3$			5.624, 44.681	1224.9	
	$TmB_{22}C_3$			5.631, 44.737	1228.7	
	$LuB_{22}C_3$			5.595, 44.464	1205.7	
15R	$YB_{28.5}C_4$	6	$R\bar{3}m$ (No. 166)	5.649, 56.899	1572.7	16
	$HoB_{28.5}C_4$			5.638, 56.881	1566.0	
	$ErB_{28.5}C_4$			5.640, 56.868	1566.5	
	$TmB_{28.5}C_4$			5.622, 56.649	1550.9	
B_4C	$B_{12}C_3$	3	$R\bar{3}m$ (No. 166)	5.601, 12.073	328.03	4

^{a} Z is the number of formulas in one unit cell. ^{b} The number of independent atoms in the asymmetry unit cell.

Results and Discussion

Figure 1 shows the schematic drawing of the crystal structures of the three phases together with that of B_4C. All of the new phases are in trigonal symmetry and with the space groups $P\bar{3}m$ for the first one and $R\bar{3}m$ for the latter two. The crystal parameters of the three phases are listed in Table 1. After comparison of their structures with B_4C, it is obvious that in the three phases it can be considered that every third, fourth, and fifth icosahedral layer in B_4C is replaced with a layer composed of boron octahedra and rare earth atoms. The stacking

(11) Zhang, F. X.; Leithe-Jasper, A.; Xu, J.; Mori, T.; Matsui, Y.; Tanaka, T.; Okada, Y. *J. Solid State Chem.* **2001**, *159*, 174.
(12) Zhang, F. X.; Xu, F. F.; Mori, T.; Liu, Q. L.; Sato, A.; Tanaka, T. *J. Alloys Compd.*, in press.
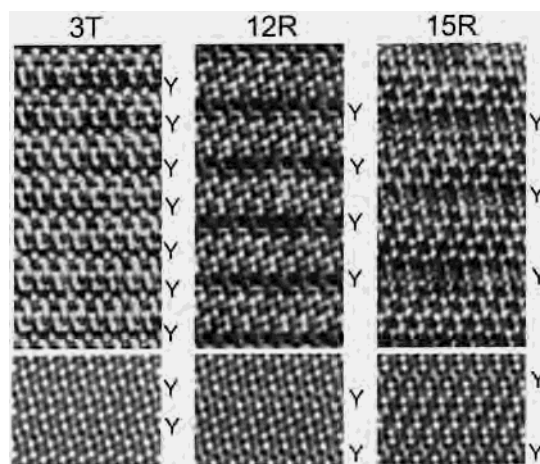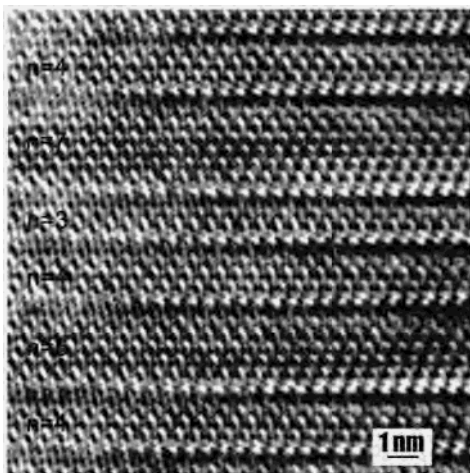
Figure 2. The observed (top row) and calculated (bottom row) high-resolution transmission electron microscope images along the [010] direction for the single phase of 3T, 12R, and 15R in the YBC(N) system. The layers marked with Y are layers composed of boron octahedra and Y atoms

sequences of the three phases are $O_1I_2I_3$, $O_1I_2I_3I_1O_2I_3I_1I_2O_3I_1I_2I_3$, and $O_1I_2I_3I_1I_2O_3I_1I_2I_3I_1O_2I_3I_1I_2I_3$, O and I representing the octahedral and icosahedral layers, respectively, and the subscript i showing boron clusters with different center positions at $(^1/_3,^2/_3,z_1)$, $(^2/_3,^1/_3,z_2)$, and $(1,1,z_3)$ for $i = 1$, 2, and 3, respectively. The first phase needs only 3 layers to obtain a periodic stacking and is called 3T (T means trigonal lattice), and the latter two are thus called 12R and 15R phases (R means rhombohedral lattice). Structural solution indicates that there are 9, 12, and 16 independent atoms in the asymmetry unit cell for the three phases, respectively. The structures and the homologous character were also confirmed by transmission electron microscopy observations. The high-resolution images of the three phases along the [010] direction in Figure 2 clearly

Figure 3. HRTEM image of the homologous phases with different stacking (stacking fault) in the YBC(N) system.

indicates the homologous character. If we set n as the number of icosahedral layers between two neighboring octahedral layers, the composition formula of the homologous phase can be written as $B_6(C_2B)_{(n-1)/2}(REC)(B_{12})_n$, where the C atom connected with Re can be replaced with N for the first two phases. For the three phases of 3T, 12R, and 15R, n equals 2, 3, and 4, respectively. It is possible to get phases with $n > 4$ in the series. In fact, different stacking schemes with n from 2 to 11 have been found by HRTEM observation. However, it is not easy to obtain any single phases with $n \geq 5$ by solid state reaction methods, because the too long c-axis will cause a stacking fault between different layers (Figure 3). However, they may be prepared by other methods, such as superlattice, which can be prepared by MBE techniques. For stacking with a large value of n, it is difficult to distinguish the new homologous phase and B_4C with impurity, because B_4C can also be included in the series only by setting n as ∞. It is interesting that, if the stacking sequence is controlled properly, we may be able to prepare new materials with a desired stacking period. Such naturally grown superlattice-like materials may have some potential applications.

Due to the structural similarity, it is interesting to study the vibrational characters of the homologous phases and compare the Raman spectra with that of B_4C. The Raman spectrum of B_4C has been widely investigated both experimentally and theoretically[13-16] due to the icosahedral cluster structure. The Raman spectrum of B_4C can be divided into two ranges, the range with two sharp peaks at 481 and 534 cm^{-1} and the range of 690−1200 cm^{-1} with broad peaks. All the peaks in the latter region are attributed to the vibrational modes of the intraicosahedral and intericosahedral bonds. The two sharp peaks in the first range are most characteristic, and their origins have been argued for a long time. Now the accepted understanding of the two peaks is that[14] the 481 cm^{-1} is the E_g mode of C−B−C chain rotating around the [111] axis of the rhombohedral unit cell (the c-axis in the hexagonal unit cell) and the latter one is attributed to the rotation of a whole boron icosahedron around
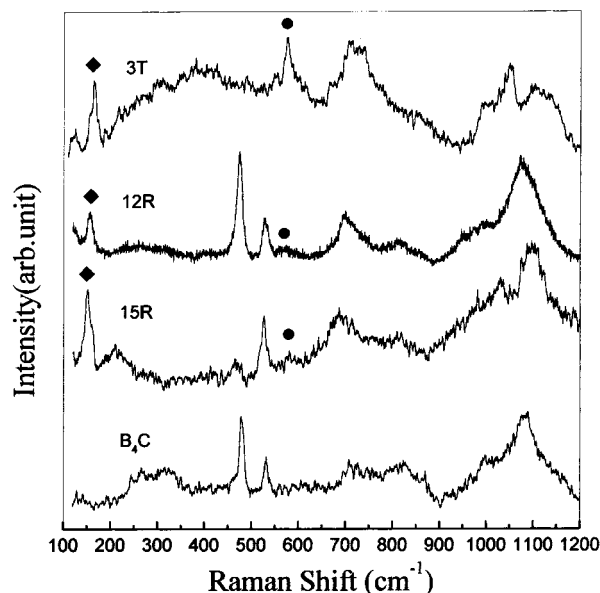

Figure 4. Raman spectra of B_4C and the homologous phases of 3T, 12R, and 15R in the YBC(N) system. The marked peaks are additional vibrational modes in the homologous phases compared with the spectrum of B_4C.

Table 2. Typical Raman Shifts of the Homologous Phases in the YBC(N) System and B_4C in the Range 100−690 cm^{-1}

phase	Raman shifts (cm^{-1})			
3T	486	575	164	574
12R	474	528	156	576
15R	474	529	152	580
B_4C	481	534		

one of the two axes orthogonal to the [111] rhombohedral axis[17] (the a- or b-axis in the hexagonal unit cell).

The Raman spectra of the homologous phases were taken in a backscattering mode using the 514 nm line of an Ar ion laser at a spectral resolution of ∼1 cm^{-1}. The Raman spectra of crystallites of the homologous phases are shown in Figure 4 together with that of B_4C. The broad peaks in the range 690−1200 cm^{-1} for the three phases are quite similar with those of B_4C, which shows the similar bonding environment of the boron icosahedron between B_4C and the other phases. However, there are some differences between B_4C and the REBC(N) systems in the low-frequency region. The Raman shifts in the low-frequency region of the phases are listed in Table 2 together with that of B_4C. The two vibrational modes of 534 and 481 cm^{-1} in B_4C still appeared in the homologous phases, only with slight frequency shifts. However, their intensity in the 3T phase is quite weak, which may be caused by the different environment of icosahedra in the 3T phase. The most obvious difference is the appearance of an additional peak with a frequency of 164, 156, and 152 cm^{-1} for the phases 3T, 12R, and 15R in the very low frequency region. They cannot be attributed to Rayleigh scattering because Rayleigh scattering only affects the spectra at frequencies lower than 100 cm^{-1} for the present apparatus and such a peak did not appear in the Raman spectrum of B_4C. We also measured the lowest frequency Raman shift for other rare earth elements in the 12R phase. The values change from 108 cm^{-1} for Lu to 120 cm^{-1} for Ho. So we can attribute the peak to the vibrational mode including heavy rare earth atoms because the frequencies hold approximately reciprocal proportionality to the masses of Y and other rare earth atoms.

(13) Tallant, D. R.; Aselage, T. L.; Campbell, A. N.; Emin, D. *Phys. Rev.* **1989**, *B40*, 5649.
(14) Lazzari, R.; Vast, N.; Besson, J. M.; Baroni, S.; Corso, A. D. *Phys. Rev. Lett.* **1999**, *83*, 3230.
(15) Vast, N.; Baroni, S.; Zerah, G.; Besson, J. M.; Polian, A.; Grimsditch, M.; Chervin, J. C. *Phys. Rev. Lett.* **1997**, *78*, 693.
(16) Nelmes, R. J.; Loveday, J. S.; Wilson, R. M.; Marshall, W. G.; Besson, J. M.; Klotz, S.; Hamel, G.; Aselage, T. L.; Hull, S. *Phys. Rev. Lett.* **1995**, *74*, 2268.

(17) Beckel, C. L.; Yousaf, M.; Fuka, M. Z.; Raja, S. Y.; Lu, N. *Phys. Rev.* **1991**, *B44*, 2535.

However, another additional peak between 570 and 580 cm^{-1} is the second difference between B$_4$C and the homologous phases. Such a peak is very strong in the case of 3T. This mode seems difficult to explain. The only difference between the three phases in REBCN systems and B$_4$C is the replacement of boron octahedral layers, so the Raman shifts between 570 and 580 cm^{-1} may be caused by the boron octahedron. The intensity of the peak seems also to support such an assumption, because the intensity in the 3T phase is the highest, in which the boron octahedron/icosahedron ratio is 1:2, also the highest in the series.

In order to measure the resistivity, polycrystalline samples of YB$_{28.5}$C$_4$ (15R) and YB$_{22}$C$_3$ (12R) were hot pressed into dense cylinders. The resistivities are plotted in Figure 5 versus the temperature to the $-1/4$ power. As temperature is lowered, resistivity increases in a straight line, following hopping behavior which has been typically observed for rare earth boron-rich solids.[18] The characteristic temperature T_0 was determined to be $T_0 = 9.3 \times 10^5$ K for YB$_{28.5}$C$_4$ and $T_0 = 8.6 \times 10^6$ K for YB$_{22}$C$_3$. The resistivity decreases as the number of layers increases from 12R to 15R approaching boron carbide.

Recently rare earth element doped Si or GaN has been intensively investigated[19−20] expecting light emissions from trivalent rare earth ions. However, the solubility of rare earth ions in them under equilibrium conditions is rather low.

Figure 5. Resistivities of YB$_{28.5}$C$_4$ ($\times$) and YB$_{22}$C$_3$ ($\bigcirc$) plotted versus the temperature to the $-1/4$ power.

Nonequilibrium doping using such methods as ion implantation can increase their contents, but lattice distortion caused by the doping used to reduce the efficiency of the light emission. Meanwhile the present homologous phases are basically semiconductors in which rare earth ions exist as the constituent element. We may be able to expect highly efficient light emission. Synthesis of thin films and measurements of semiconducting and light emission properties are in preparation.

IC010527S

(18) Dzhamagidze, S. Z.; Malttsev, Y. A.; Shvangiradze, R. R. *Fiz. Tekh. Poluprov.* **1968**, *2*, 387.
(19) Coffa, S.; Franzo, G.; Priolo, F. *MRS Bull.* **1998**, *23*, 25.
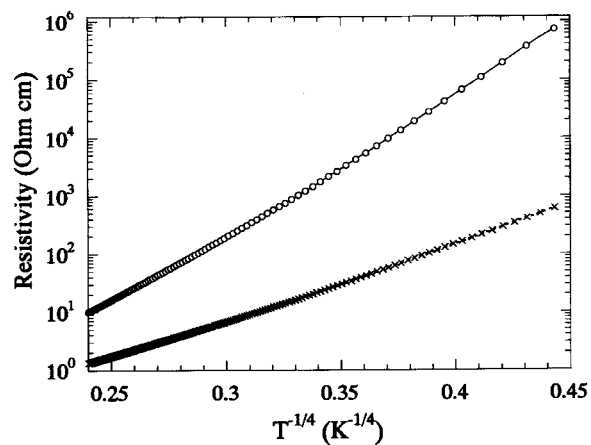(20) Steckl, A. J.; Zavada, J. M. *MRS Bull.* **1999**, *24*, 33.